Polyaniline Nanofibers Supported on Titanium as Templates for Immobilization of Pd Nanoparticles: A New Electro-Catalyst for Hydrazine Oxidation

M. G. Hosseini,[1] S. Zeynali,[1] M. M. Momeni,[1] R. Najjar[2]

[1]Department of Physical Chemistry, Electrochemistry Research Laboratory University of Tabriz, Tabriz, Iran
[2]Department of Organic Chemistry, Polymer Research Laboratory, University of Tabriz, Tabriz, Iran

ABSTRACT: Palladium nanoparticles (Pd-NPs)/polyaniline (PAni)/titanium (Ti) catalysts were prepared using electroless deposition of Pd-NPs on PAni matrixes coated on Ti substrate. PAni/Ti electrodes were synthesized by electro-polymerization of aniline on Ti. The morphology of Pd-NPs on PAni/Ti electrodes were characterized by scanning electron microscopy technique and results indicated that Pd-NPs were uniformly dispersed on the surface of PAni film. The electro-catalytic properties of Pd-NPs/PAni/Ti catalysts toward oxidation of hydrazine were investigated by different electrochemical methods and results showed that Pd-NPs/PAni/Ti catalysts have high electrochemical activity. In addition, the mechanism of hydrazine electrochemical oxidation catalyzed by Pd-NPs/PAni/Ti was investigated. © 2011 Wiley Periodicals, Inc. J Appl Polym Sci 124: 4671–4677, 2012

Key words: conducting polymers; palladium nanoparticles; electro-polymerization; polyaniline; direct hydrazine fuel cells

INTRODUCTION

The development of inorganic/organic composites has recently received increasing attention due to their wide range of potential uses. Composites of conducting polymers and inorganic nanoparticles have received a lot of attention because of their usefulness in several applications.[1–4] Various approaches have been used to prepare conducting polymer/metal composites. Many studies have been devoted to the dispersion of metal particles in thin films of electro-inactive polymers,[5,6] redox polymers,[7–9] and conducting polymers.[10,11] Among these polymers, polyaniline (PAni) is one of the most important conducting polymers because of its high conductivity, ease of preparation, good environmental stability, and large variety of applications such as electro-chromic devices, secondary batteries, catalysis, and corrosion protection coatings.[12–14]

Direct methanol fuel cell is expected as a hopeful candidate for direct fuel cell application systems. However, the efficiency and power output of direct methanol fuel cells are low because of severe poisoning of the anode catalyst by reaction intermediates such as CO.[15] Hydrazine is an important high-performance fuel in aerospace propulsion applications, which also impresses promising potential applications in fuel cells. Hydrazine is an ideal fuel for a direct fuel cell system because it does not exhaust environmentally loading materials such as CO_2. Hydrazine is a compound with high hydrogen content (12.5 wt %). Its hydrogen storage capability is higher than that of sodium borohydride (10.6 wt %) and equivalent to that of methanol. The direct hydrazine fuel cell demonstrates a higher electromotive force of 1.61 V which is close to that of the direct borohydride fuel cell (1.64 V) and higher than that of the direct methanol fuel cell (1.21 V). When hydrazine is used as a fuel to power the direct hydrazine fuel cell, only nitrogen and water will be formed. However, specific precautions should be observed when using hydrazine solution as a fuel for the direct hydrazine fuel cell because hydrazine is toxic and carcinogenic compound.[16] The direct hydrazine fuel cell concept was first suggested in the 1960s.[17] Very few researches on the direct hydrazine fuel cell development have been done.[18–21] It is considered that more attentions should be paid to develop the direct hydrazine fuel cell technology due to the merits mentioned above. Noble metals such as platinum,[22] palladium,[23,24] silver,[25] and gold[26,27] are very active in the anodic oxidation of hydrazine. However, they tend to lose reactivity as they precipitate or form a surface film. Immobilization

of the noble metal nanoparticles in an active matrix may enhance the overall reactivity of the catalytic metal centers. For example, our recent studies have shown that the immobilization of the metal nanoparticles in an active matrix improves the electro-catalytic activity to a great extent.[28–33] The aim of this study was to investigate the electro-oxidation of hydrazine on Pd-NPs dispersed in PAni matrices and analyze the effect of their morphologies on the electro-catalytic characteristics of this modified electrode. The PAni films were obtained by electro-polymerization of aniline on titanium (Ti) substrates. Pd-NPs dispersed on the PAni films by electroless deposition. The electro-oxidation of hydrazine on Pd-NPs/PAni/Ti electrodes was carried out using cyclic voltammetry methods.

EXPERIMENTAL

Solutions, chemicals, and electrochemical measurement

Hydrazine (Merck, >99%) and H_2SO_4 (Merck, >99%) were used as received. All other chemicals were of analytical grade and used without further purification. Aniline was distilled under reduced pressure and then stored at low temperature before use. All electrochemical experiments were carried out at room temperature. Distilled water was used throughout. The electrochemical experiments were performed in a three-electrode cell assembly. A platinum sheet of the geometric area of about 20 cm^2 was used as counter electrode, while all potentials were measured with respect to a commercial saturated calomel electrode (SCE). Electrochemical experiments were carried out using a Princeton Applied Research, EG&G PARSTAT 2263 Advanced Electrochemical System run by Power-Suite Software.

Electro-polymerization of polyaniline on titanium (PAni/Ti electrodes)

Electro-polymerization of PAni from an acidic solution was conducted on Ti electrode. Ti discs were cut from a Ti sheet (purity 99.99%, 1 mm thickness) and mounted using polyester resin. The deposition of conducting polymers on spontaneously passivating metals such as Ti and aluminum usually requires a pre-treatment of the substrate to remove natural oxides, which cover the metal surface. Prior to electro-polymerization of aniline, the Ti electrodes were first mechanically polished with different grades of abrasive papers, rinsed in a run of distilled water, then chemically etched by immersing in a mixture of volumetric 1 : 4 : 5 of HF : HNO_3 : H_2O. The last step of pretreatment was rinsing with

deionized water. After the pretreatment, electro-polymerization of aniline was conducted in a solution containing of $0.1M$ aniline $+ 0.5M$ H_2SO_4 under galvanostatic conditions with a current density of 10 mA cm^{-2} for 10 min. The temperature is maintained at 25°C.

Preparation of Pd-NPs/PAni/Ti catalysts

After rinsing with water, the PAni/Ti electrodes were immerged into the bath for deposition of palladium on result PAni. Pd-NPs were deposited on PAni/Ti electrodes by electroless method. The sensitizing-activating treatment was carried out by soaking them first in 0.0045 mol L^{-1} $SnCl_2$ solution for 2 min and then in 0.00059 mol L^{-1} $PdCl_2$ solution for 4 min at room temperature. The samples were then rinsed with distilled water and soaked in the electroless-plating bath containing 0.01 mol $PdCl_2$, 4.8 g L^{-1} of ethylene-diamine as a complexing agent, and 11 g L^{-1} of $N_2H_4.H_2O$ as a reducing agent, while pH value was adjusted to 8 with HCl and NaOH. The reaction temperature was 323 K. All mentioned processing performed in an ultrasonic bath. Electroless deposition of palladium on PAni/Ti supports was performed in various times and finally it was observed that 5 min is the optimum time, resulting in highest current values. After the electroless plating, the samples were rinsed, dried, and subjected to the characterization.

Determination of electrode surface area

The area of the Pd-NPs/PAni/Ti electrode was determined using 1 mM $K_4Fe(CN)_6$ in $0.1M$ KNO_3 electrolyte by recording the cyclic voltamograms. From the cyclic voltammetric peak current and the diffusion coefficient of hexacyanoferrate, the area of the electrode was calculated by using the equation[34]:

$$i_{pa} = (2.69 \times 10^5)n^{3/2}AD_o^{1/2}v^{1/2}C_o^*   \qquad (1)$$

where n is the number of electrons transferred, that is, in this Case 1; A is surface area of the electrode; D_o is the diffusion coefficient (9.382×10^{-6} cm^2 s^{-1}); v is the scan rate (0.1 V s^{-1}), C_o^* is the concentration of electro-active species (1 mM). The surface area of Pd-NPs/PAni/Ti electrode was estimated to be about eight times of flat palladium electrode.

Characterization of morphology

For characterizing morphology and composition of PAni coating on Ti electrode and Pd-NPs on the PAni films, a scanning electron microscope (Model XL30, Philips, Netherlands) was employed with an accelerating voltage 30 kV. To identify the element composition, an energy dispersive X-ray (EDX
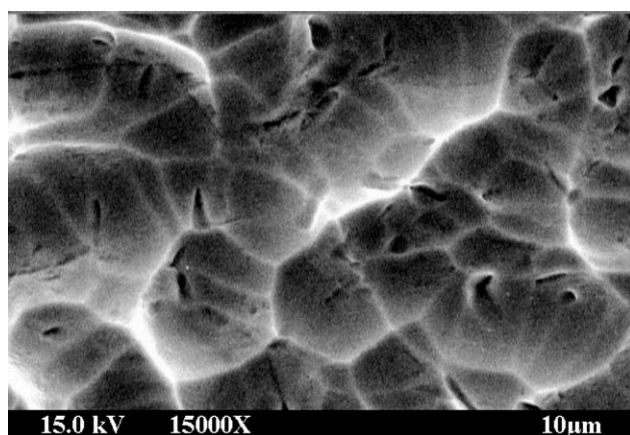
Figure 1 SEM image of titanium substrate before deposition of PAni film on it.

Genesis fitted to the Philips SEM XL30) analysis was carried out.

RESULTS AND DISCUSSION

Morphology of PAni/Ti and Pd-NPs/PAni/Ti electrodes

Figure 1 shows SEM micrograph of the surface of Ti substrate before deposition of PAni film on it. It can be seen that Ti substrate was smooth and planar before depositing the film on it. SEM images of the pure PAni film (without deposited palladium) obtained by electro-polymerization with different magnifications are shown in Figure 2(a,b). PAni films synthesized by galvanic polymerization are distributed uniformly on the surface of the Ti electrode and have a high surface area, thus making them ideal for use as a good support.

Figure 3 shows the SEM micrographs of Pd-NPs deposited on the PAni film. It can be seen that the Pd-NPs are distributed at the surface of the PAni film. Figure 4 shows the energy dispersive X-ray (EDX) spectrum of Pd-NPs/PAni/Ti electrodes. EDX results confirm the presence of palladium particle in the surface.

Characterization of the Pd-NPs/PAni/Ti electrode

To determine whether the deposition procedure had resulted in the removal of the surface oxide layer, thereby ensuring good electrical contact between the palladium and PAni coating and the underlying Ti electrode, the Pd-NPs/PAni/Ti were tested as electrodes using a one electron redox couple. Figure 5 shows the voltammetric curves for the reduction of $K_3Fe(CN)_6$ on Pd-NPs/PAni/Ti, flat palladium and bare Ti electrodes. The voltammogram for the Pd-NPs/PAni/Ti electrode shows the expected

reversible behavior for the reduction on a bulk palladium electrode. In comparison, the voltammogram obtained with one Ti electrode shows increased peak separation and peak widths. This is probably attributable to a passivating surface film, most likely the oxide layer present on the surface of the Ti electrode. It has been reported in the literature that on exposure to air, a thin Ti oxide film is formed on the surface of a Ti layer.[28] This could grow thicker, as well as becoming an Ti oxide layer when using Ti as an electrode, due to electrochemical (or chemical through ferricyanide) oxidation. The presence of such a passivating layer would be expected to produce the observed small change in the standard redox potential as well as a significant iR drop in the resistive surface layer, which would shift the position of the peaks for the redox reaction of the ferri/ferrocyanide to greater overpotentials, increasing peak separation and reducing peak heights, as observed. The lack of such resistances and overpotentials observed on repeated redox cycling of the Pd-NPs/PAni/Ti electrode indicates that there is no significant resistive film (either initially present or developing with cycling) between the underlying Ti and the palladium and PAni coating film.
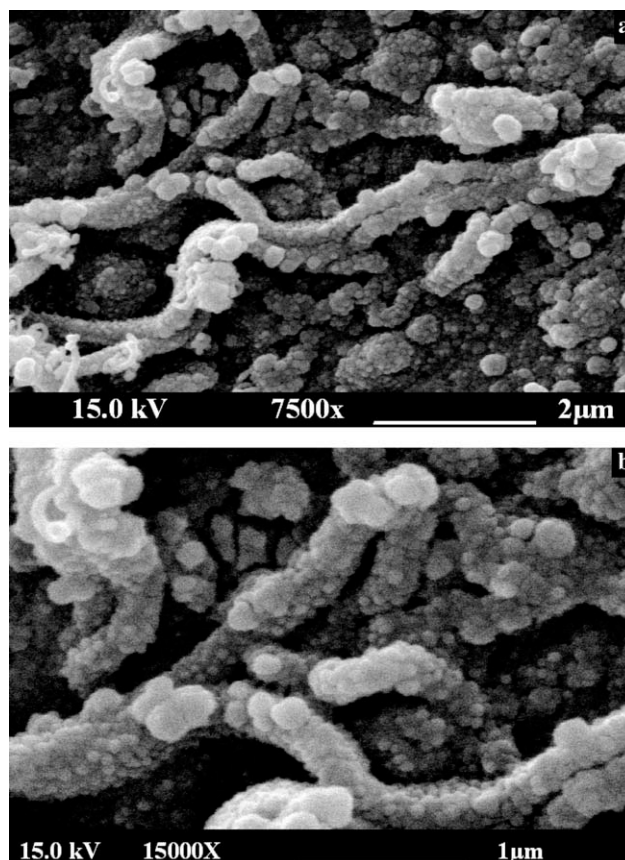

Figure 2 SEM images of pure PAni film (without deposited palladium) on the titanium electrode with different magnifications (a,b).
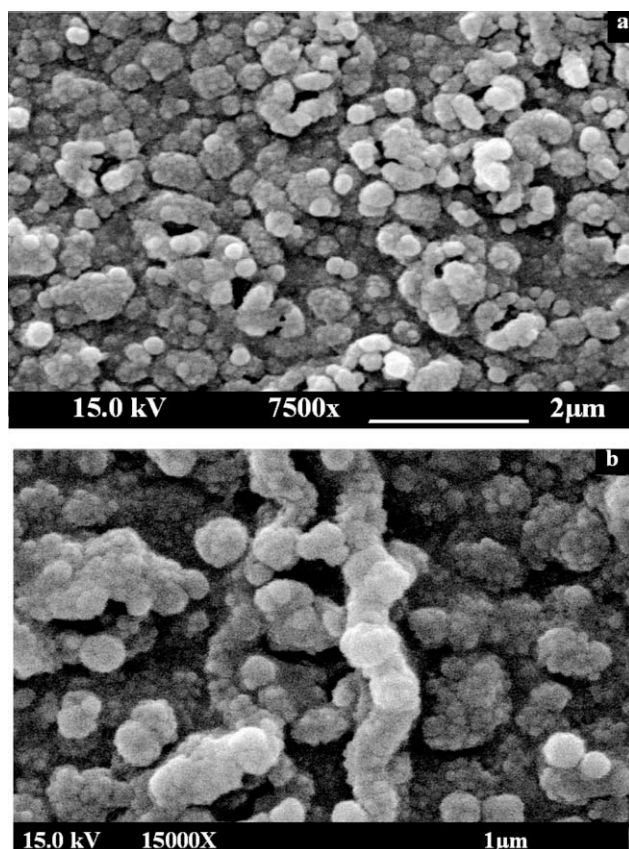
Figure 3 SEM images of Pd-NPs deposited on the PAni film with different magnifications (a,b).

Cyclic voltammetric study of hydrazine electro-oxidation on the electrodes

To compare Pd-NPs/PAni/Ti electrode with Ti electrode, the method of cyclic voltammetry was used to follow the electro-catalytic behavior of the electro-
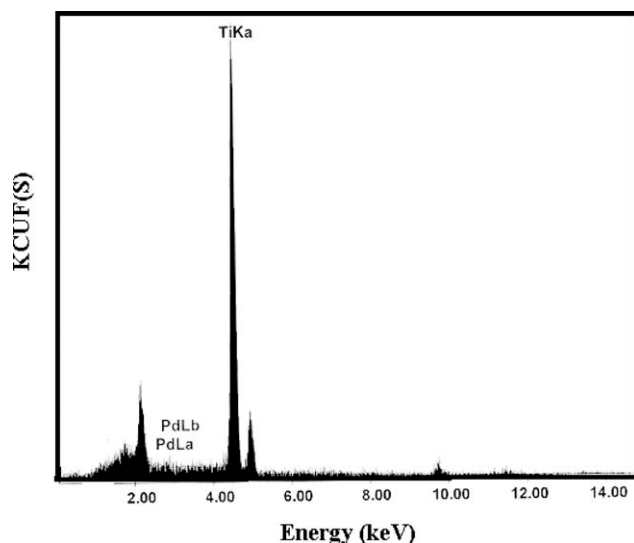

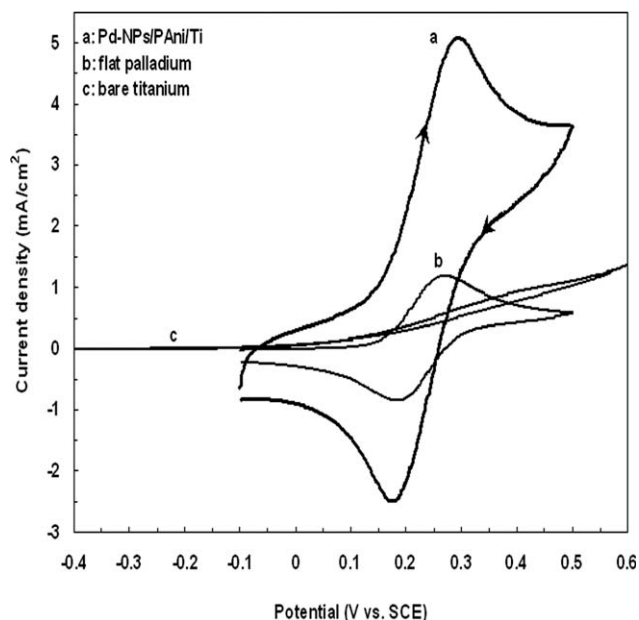**Figure 4** Energy dispersive X-ray (EDX) of Pd-NPs/PAni/Ti electrode.

Figure 5 Cyclic voltammograms for Pd-NPs/PAni/Ti (1×1 cm^2), flat palladium (1×1 cm^2), and bare titanium (1×1 cm^2) electrodes, recorded at 100 mV s^{-1} in a solution containing 10 mM K$_3$[Fe(CN)$_6$] in 1M KCl at 25°C.

des. Figure 6(a) presents cyclic voltammograms of Ti and Pd-NPs/PAni/Ti electrodes in 0.5M H$_2$SO$_4$ + 1 mM hydrazine aqueous solution, at a scan rate of 100 mV s^{-1}. The pure Ti electrode exhibited no oxidation peak for hydrazine but after replacing the pure Ti electrode with Pd-NPs/PAni/Ti electrode, distinguished peaks were observed in the cyclic voltammetry, therefore confirming the Pd-NPs/PAni/Ti electrodes electro-catalytic activity. Figure 6(b) presents cyclic voltammograms of flat palladium and Pd-NPs/PAni/Ti electrodes in 0.5M H$_2$SO$_4$ + 1 mM hydrazine aqueous solution, at a scan rate of 100 mV s^{-1}. The current density for hydrazine oxidation on Pd-NPs/PAni/Ti electrode is greater than that observed for palladium electrode. This result may be attributed to the larger specific surface area of the Pd-NPs/PAni/Ti electrodes.

Effect of scan rate

The effect of different scan rates on the electro-catalytic properties of Pd-NPs/PAni/Ti electrode towards hydrazine oxidation has been studied and results were shown in Figure 7. As can be seen from Figure 7, the increase in potential scan rate induced an increase in the electro-catalytic peak current and resulted in a shift to more positive potential value for the catalytic oxidation of hydrazine. This clear shift of the peak potential was occurred as expected for irreversible electrochemical reactions.[35]
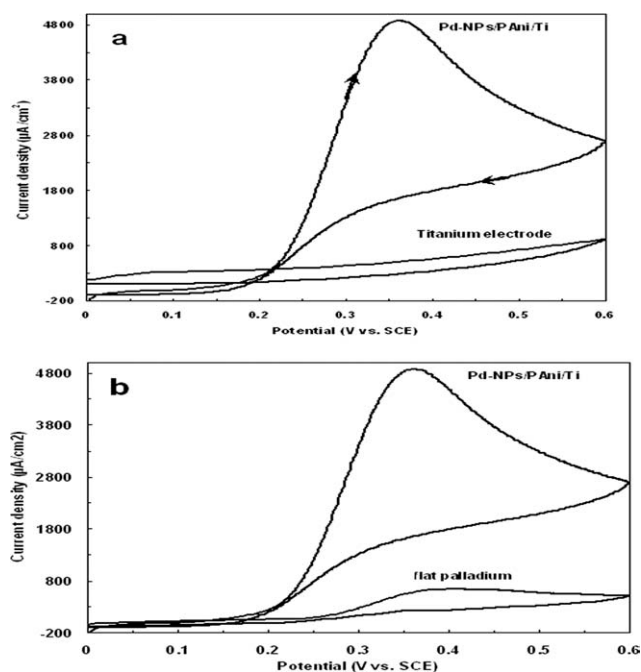
Figure 6 (a) Cyclic voltammograms for Pd-NPs/PAni/Ti and bare titanium electrodes in $0.5M$ H_2SO_4 + 1 mM hydrazine aqueous solution at 25°C with a scan rate of 100 mV s^{-1}. (b) Cyclic voltammograms for Pd-NPs/PAni/Ti and flat palladium electrodes in $0.5M$ H_2SO_4 + 1 mM hydrazine aqueous solution at 25°C with a scan rate of 100 mV s^{-1}.

To investigate the electro-catalytic reaction mechanism of hydrazine oxidation on Pd-NPs/PAni/Ti electrode, diagram of peak current i_p versus square root of sweep rate $v^{1/2}$ was constructed. As known
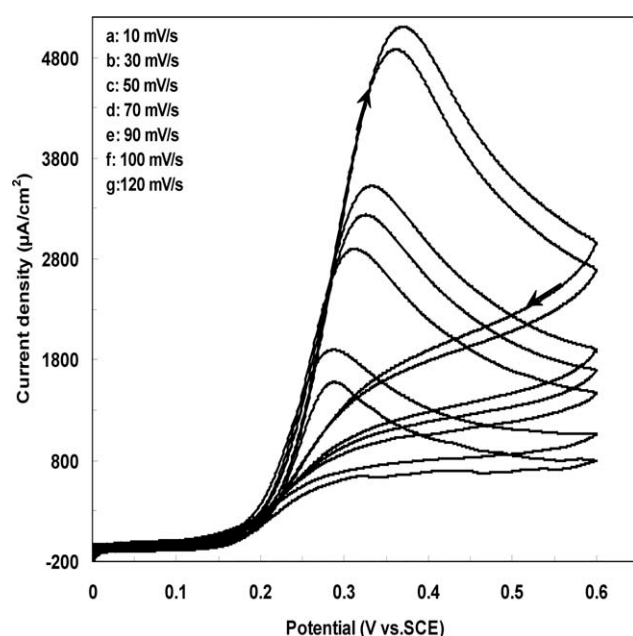

Figure 7 The cyclic voltamogrames for Pd-NPs/PAni/Ti electrode in $0.5M$ H_2SO_4 + 1 mM hydrazine aqueous solution at different scan rate.
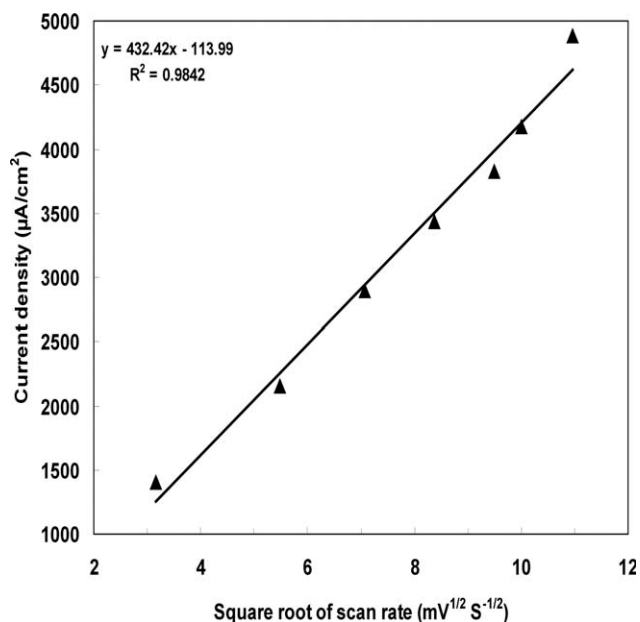

Figure 8 The plot of hydrazine oxidation peak current on the Pd-NPs/PAni/Ti electrode versus $v^{1/2}$.

in the precondition semi-infinite linear diffusion, peak current i_p was related to scan rate through the following equation:

$$i_p = (2.69 \times 10^5)n(\alpha n_a)^{1/2}AC_oD_o^{1/2}v^{1/2} \qquad (2)$$

where i_p is the peak current, v is the scan rate, n is the number of electrons transferred, α is the coefficient of electron transfer, C_o is the bulk concentration of substrate, D_o is the diffusion coefficient, and A is the electrode surface area.

If the concentration C_o is hold constant, then the peak current i_p is linearly proportional to the square root of sweep rate $v^{1/2}$. While the sweep rate is kept constant, the peak current i_p is linearly proportional to the concentration C_o, which indicates the reaction is controlled by diffusion. It is seen from Figure 8 that the peak current i_p is linearly related to the square root of sweep rate $v^{1/2}$ and the correlation coefficient is $R^2 = 0.98$, which ensures that the oxidation process of hydrazine on the Pd-NPs/PAni/Ti electrode is controlled by diffusion.

To get the information on the rate determining step, Tafel slope, b, was determined using the following equation valid for a totally irreversible diffusion controlled process[36]:

$$E_p = 0.5b \log v + \text{constant} \qquad (3)$$

Therefore, on the basis of eq. (3), the slope of E_p versus log v plot is:
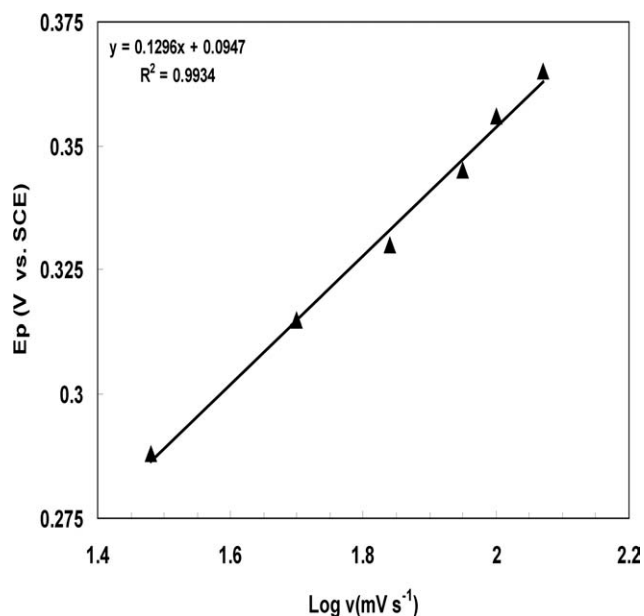
$$dE_p/d \log v = b/2 \qquad (4)$$

Figure 9 The peak potential dependence on log v for the oxidation of hydrazine at the Pd-NPs/PAni/Ti electrode.

where b is the Tafel slope and v is the scan rate; the Tafel slope can also be expressed as:

$$b = 2.3\, RT (\alpha_a n_a F)^{-1} \qquad (5)$$

On the basis of these equations, the slope of the plots of E_p versus log v is $b/2$ which was found equal to 0.129 in this work (Fig. 9), so, $b = 0.258$ V. It is known that hydrazine oxidation kinetics on many materials[37,38] occur with single electron transfer
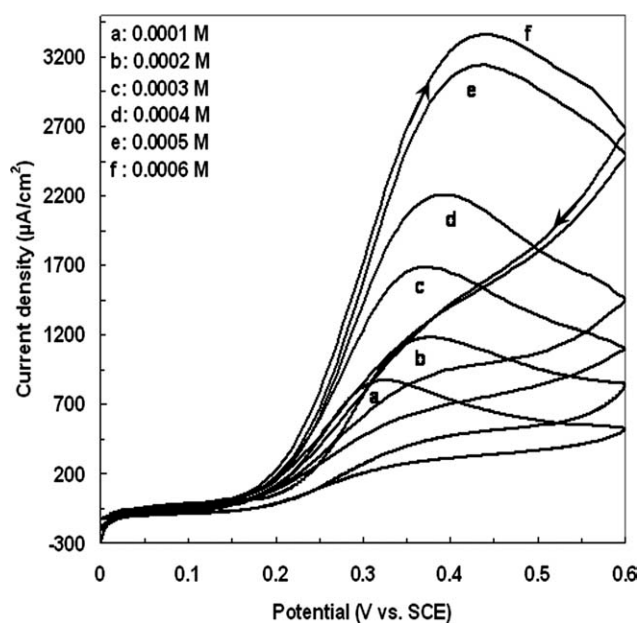

Figure 10 The cyclic voltamogrames of Pd-NPs/PAni/Ti electrode in 0.5M H$_2$SO$_4$ solution with different concentrations of hydrazine.
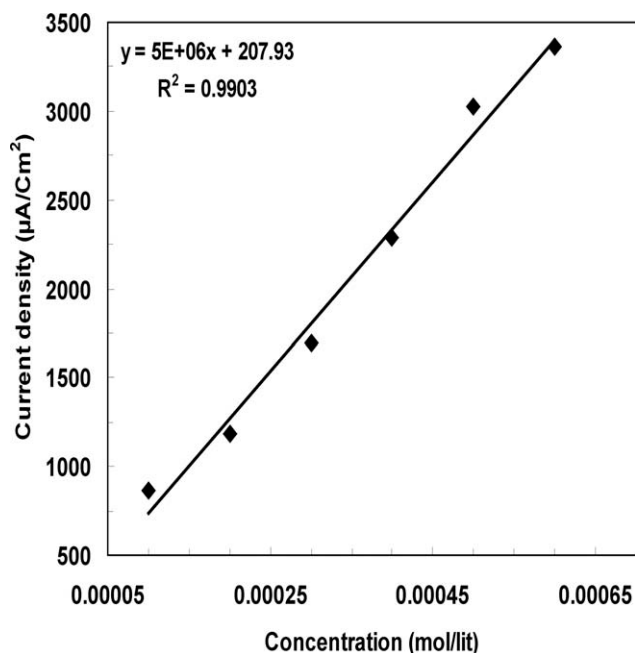
Figure 11 The plot of hydrazine oxidation peak current on the Pd-NPs/PAni/Ti electrode versus concentration of hydrazine.

process. Assuming this, these slope values indicate a transfer coefficient (α) equal to 0.197.

Electro-catalytic determination of hydrazine

Effect of hydrazine concentration on electro-catalytic response of Pd-NPs/PAni/Ti electrode was investigated by the method of cyclic voltammetry. Figure 10 shows cyclic voltammograms of the Pd-NPs/PAni/Ti electrode at the presence of various concentrations of hydrazine. The observed anodic peak current increases with increasing hydrazine concentration in the solution. This catalytic peak current shown a linear relationship with the concentration of hydrazine in the range of 2–5 mM with a correlation coefficient of $R^2 = 0.99$ (Fig. 11). From these results, it can be concluded that the electro-oxidation of hydrazine on these new modified electrodes can be used for the quantitative determination of hydrazine in samples.

CONCLUSION

A novel synthesis route for preparing Pd-NPs dispersed uniformly on the surfaces of PAni/Ti electrode has been developed with the aim of the electro-oxidation of hydrazine. The electro-catalytic activity of the Pd-NPs/PAni/Ti electrodes and pure Ti toward hydrazine oxidation was evaluated through cyclic voltammetry. The electro-chemical evaluations showed that PAni/Ti electrodes modified with Pd-NPs are highly active for electro-catalytic

oxidation of hydrazine. The oxidation kinetic of hydrazine was also studied by varying the potential scan rate. The results indicated that the oxidation process is mass transfer controlled. Finally, the oxidation current of hydrazine Pd-NPs/PAni/Ti electrodes was used for the determination of hydrazine in aqueous solution and a linear calibration curve was found in the range of 1.0–4.0 m*M* with a correlation coefficient of 0.99.

References

1. Ward, R. E.; Meyer, T. Y. Macromolecules 2003, 36, 4368.
2. Patil, R. C.; Radhakrishnan, S.; Pethkar, S.; Vijaymohanan, K. J. Mater Res 2001, 16, 1982.
3. Drury, A.; Chaure, S.; Kroell, M.; Nicolosi, V.; Chaure, N.; Blau, W. J. Chem Mater 2007, 19, 4252.
4. Feng, X. M.; Mao, C. J.; Yang. G. Hou, W. H.; Zhu, J. J. Langmuir 2006, 22, 4384.
5. Kao, W. H.; Kuwana, T. J. Am Chem Soc 1984, 106, 473.
6. Bartak, D. E.; Kazee, B.; Kuwana, T. Anal Chem 1990, 62, 151.
7. Tourillon, G.; Garnier, F. J Phys Chem 1984, 88, 5281.
8. Chandler, G. K.; Pletcher, D. J Appl Electrochem 1986, 16, 62.
9. Leone, A.; Marino, W.; Scharifker, B. R. J Electrochem Soc 1992, 139, 438.
10. Coche, L.; Moutet, J. C. J Am Chem Soc 1987, 109, 6887.
11. Takano, N.; Kawakami, Y.; Takeno, N. Chem Lett 1996, 8, 589.
12. Zhang, L. J.; Wan, M. X. J Phys Chem B 2003, 107, 6748.
13. Liang, L.; Liu, J.; Windisch, C. F.; Exarhos, G. J.; Lin, Y. Angew Chem Int Ed 2002, 41, 3665.
14. Hosseini, M. G.; Sabouri, M.; Shahrabi, T. J Appl Polym Sci 2008, 110, 2733.
15. Ren, X.; Wilson, M. S.; Gottesfeld, S. J Electrochem Soc 1996, 143, L12.
16. Lamy, C.; Leger, J. M. In Proceedings of the First International Symposium on New Material Fuel Cell Systems, 1995; Vol. 296.
17. Yin, W. X.; Li, Z. P.; Zhu, J. K.; Qin, H. Y. J Power Sources 2008, 182, 520.
18. Bard, A. J Anal Chem 1963, 35, 1602.
19. Yamada, K.; Yasuda, K.; Fujiwara, N.; Siroma, Z.; Tanaka, H.; Miyazaki, Y.; Kobayashi, T. Electrochem Commun 2003, 5, 892.
20. Asazawa, K.; Yamada, K.; Tanaka, H.; Oka, A.; Taniguchi, M.; Kobayashi, T. Angew Chem Int Ed 2007, 46, 8024.
21. Yamada, K.; Yasuda, K.; Tanaka, H.; Miyazaki, Y.; Kobayashi, T. J Power Sources 2003, 122, 132.
22. Yin, W. X.; Li, Z. P.; Zhu, J. K.; Qin, H. Y. J Power Sources 2008, 182, 520.
23. Dong, B.; He, B. L.; Huang, J.; Gao, G. Y.; Yang, Z.; Li, H. L. J Power Sources 2008, 175, 266.
24. García Azorero, M. D.; Marcos, M. L.; González Velasco, J. Electrochim Acta 1994, 39, 1909.
25. Li, F.; Zhang, B.; Wang, E.; Dong, S. J Electroanal Chem 1997, 422, 27.
26. Guo, D.; Li, H. J Colloid Interface Sci 2005, 286, 274.
27. Guo, D.; Li, H. Electrochem Commun 2004, 6, 999.
28. Hosseini, M. G.; Sajjadi, S. A. S.; Momeni, M. M. Surf Eng 2007, 23, 419.
29. Hosseini, M. G.; Momeni, M. M.; Faraji, M. J Appl Electrochem 2010, 40, 1421.
30. Hosseini, M. G.; Sajjadi, S. A. S.; Momeni, M. M. IUST Int J Eng Sci 2008, 7, 39.
31. Hosseini, M. G.; Momeni, M. M. J Mater Sci 2010, 45, 3304.
32. Hosseini, M. G.; Momeni, M. M.; Faraji, M. J Mater Sci 2010, 45, 2365.
33. Hosseini, M. G.; Momeni, M. M.; Faraji, M. J Mol Catal A Chem 2011, 335, 199.
34. Gosser, D. K. Cyclic Voltammetry; VCH: New York, 1994.
35. De la Fuente, C.; Acuna, J. A.; Vasquez, M. D.; Tascon, M. L.; Gomez, M. I.; Batanero, P. S. Talanta 1997, 44, 685.
36. Pournaghi-Azar, M. H.; Razmi-Nerbin, H. J Electroanal Chem 2000, 488, 17.
37. Ardakani, M. M.; Ebrahimi karaim, P.; Rahimi, P.; Zare, H. R.; Naeimi, H. Electrochim Acta 2007, 52, 6118.
38. Ozoemena, K. I.; Nyokong, T. Talanta 2005, 67, 162.